*Article*

# Inner-Shell Ionization and Fragmentation of Isolated Endohedral Fullerene Ions by XUV Radiation †

**Stefan Schippers**

I. Physikalisches Institut, Justus-Liebig-Universität Gießen, Heinrich-Buff-Ring 16, 35392 Gießen, Germany; stefan.schippers@physik.uni-giessen.de

† This paper is an extended version of my paper given at the 13th International Conference on Atomically Controlled Surfaces, Interfaces and Nanostructures (ACSIN2016), Rome, Italy, 9–15 October 2016.

**Abstract:** The photon–ion merged-beams technique for photoabsorption studies of ionized nanoparticles with synchrotron radiation is introduced. As an example, recent results from photoionization and photofragmentation of the endohedral fullerene ions $Lu_3N@C_{80}^+$, $Lu_3N@C_{80}^{2+}$, and $Lu_3N@C_{80}^{3+}$ are briefly discussed, highlighting the sensitivity and versatility of the experimental technique.

## 1. Introduction

Endohedral fullerenes are fascinating objects that have captured the imagination of many scientists. Their special molecular structure of a closed carbon cage surrounding an encapsulated atom or molecule has given rise to many intriguing ideas in the basic and applied sciences. Examples are the use of endohedral fullerenes in photovoltaics, quantum computing, medical imaging, or tumor therapy (see [1] for a recent comprehensive review). So far, most of the research on endohedral fullerenes has been theoretical in nature. Experiments were rather limited, mainly because the chemical synthesis of endohedral fullerenes is complicated, such that large quantities of high purity material are not readily available. This largely prevented the use of neutral endohedral fullerene vapour as a gas target (e.g., for photoabsorption experiments). A few attempts are documented in the literature ([2] and references therein), but these did not yield very conclusive results. In addition, a number of studies have been reported where endohedral fullerenes were prepared as thin films on solid surfaces (see [1] for further details).

As compared to spectroscopy of a neutral gas target, the photon-ion merged-beams technique (see [3] for a recent introductory review and Section 2 below) is a significantly different experimental approach which also permits sensitive measurements of photo-ion yields when only small amounts of low-purity sample material are available. Based on previous experience with empty fullerenes [4–6], a Gießen–Reno–Advanced Light Source (ALS) collaboration applied the photon-ion merged-beams method successfully for photoionization and photofragmentation studies with the endohedral fullerene ions $Sc_3N@C_{80}^+$ [7], $Ce@C_{82}^+$ [8], and $Xe@C_{60}^+$ [9,10]. The scientific issues that were addressed in these studies with empty and filled fullerenes comprised collective excitations of the carbon cage, screening effects, the absorption strength of the encapsulated atom or molecule, the stability of endohedral fullerenes upon photon impact, branching ratios into the most significant fragmentation channels, charge transfer from the encaged atom to the carbon cage, and the existence of confinement resonances (a quantum mechanical multi-path interference phenomenon closely related to Extended X-ray Absorption Fine-Structure—EXAFS).

All of these previous studies were confined to photon energies below 200 eV, and only outer atomic shells were addressed. Here, recent first results on deep inner-shell photoionization and photofragmentation of $Lu_3N@C_{80}$ endohedral fullerene ions [11] are featured. The results were obtained at the new photon-ion spectrometer PIPE (Photon-Ion Spectrometer at PETRA III) [12] at the beamline P04 [13] of the synchrotron light source PETRA III in Hamburg, Germany. This beamline offers record-high photon flux in the 250–3000 eV photon-energy range and, therefore, facilitates ionization of the carbon and nitrogen K-shells, as well as the lutetium M-shell. This enables one to address the atomic species of the carbon cage as well as of the encapsulated molecular complex separately by scanning the photon energy across the ranges of the corresponding absorption edges. In this respect, the photon-ion merged-beams technique is very similar to Near-Edge X-ray Absorption Fine Structure (NEXAFS) [14] and, in the same way, allows the chemical environment of the atomic species under study to be probed.

## 2. Experimental Method

Figure 1 shows a sketch of the photon-ion merged-beams setup PIPE [12]. This setup is a permanently installed user facility at the variable polarization Extreme Ultra-Violet (XUV) beam line P04 [13] of the PETRA III synchrotron light source operated by DESY in Hamburg, Germany. The heart of the apparatus is the photon-ion merged-beams interaction region (labelled "MB" in Figure 1), where an ion beam is travelling on the same axis as the photon beam. The length of the overlap region is 1.7 m. In this way, a large interaction volume is created that at least partly makes up for the extreme diluteness of the ion-beam target. Another asset of the merged-beams technique is that the heavy photo products that are created in the photon-ion interaction region are moving all in the same direction together with the primary keV-ion beam. PIPE uses a double-focussing dipole magnet (labelled "DM" in Figure 1) to separate the various product ions and the primary ions according to their mass-to-charge ratio. At the same time, the magnet directs the selected product particles onto a single ion detector which counts these with practically 100% efficiency (due to their kinetic energies of a few keV). The combination of a large interaction volume, a record-high photon flux (more than $10^{12}$ s$^{-1}$ at 0.01% bandwidth across the entire 250–3000 eV energy range), and a highly-efficient and largely background-free product detection scheme provides a world-unique sensitivity for photon-interaction studies with ionized matter in the gas phase.

For the preparation of $Lu_3N@C_{80}^+$, $Lu_3N@C_{80}^{2+}$, and $Lu_3N@C_{80}^{3+}$ ion beams, a commercially available (in milligram quantities) mix of $Lu_3N@C_{80}$ (35%) and other fullerenes (65%, mostly $C_{60}$) was evaporated inside an Electron Cyclotron Resonance (ECR) ion source where the molecules were ionized by electron bombardment, with the electrons being heated by an externally generated 10-GHz microwave. Although such ion sources were developed specifically for the production of multiply charged ions [15], they are (when operated at low microwave power) also advantageous for the production of endohedral fullerene ions, since they are working at a comparatively low gas pressure such that precious sample material is consumed at a very low rate.

Positively charged ions were extracted from the ion source by putting the entire source on an electric potential of +6 kV. The extracted ion beam contained a mixture of molecular ions due to the presence of a considerable amount of unwanted sample material ($C_{60}$ and heavier fullerenes), and due to molecular fragmentation occurring in the ion source. The composition of the primary beam is analyzed in the same way as the composition of the product beam, i.e., by passing the primary beam through a mass/charge analyzing dipole magnet (labelled "AM" in Figure 1) located upstream of the merged-beams interaction region.

Mass-over-charge spectra of the primary ion-beam were obtained by monitoring the ion current in a Faraday cup while ramping the magnetic field. An example is shown in Figure 2. This mass/charge spectrum was taken after several days of outgassing and moderate heating of the sample. During this period of time, most lighter fractions of the sample evaporated. Therefore, the mass/charge spectrum primarily exhibits mass/charge peaks due to singly, doubly, and triply charged intact $Lu_3N@C_{80}$ ions

as well as peaks corresponding to molecular fragment ions (e.g., $Lu_2N@C_{80}^+$). In addition, there are prominent peaks of $C_{60}^+$ and $C_{60}^{2+}$. It is important to note that the individual ion species are clearly separated. If required, isotopic mass resolution can be easily achieved [10,12]. For the photoionization and photofragmentation experiments discussed below, pure beams of $Lu_3N@C_{80}^+$ and $Lu_3N@C_{80}^{2+}$ were selected for further transport to the photon-ion merged-beam interaction region.
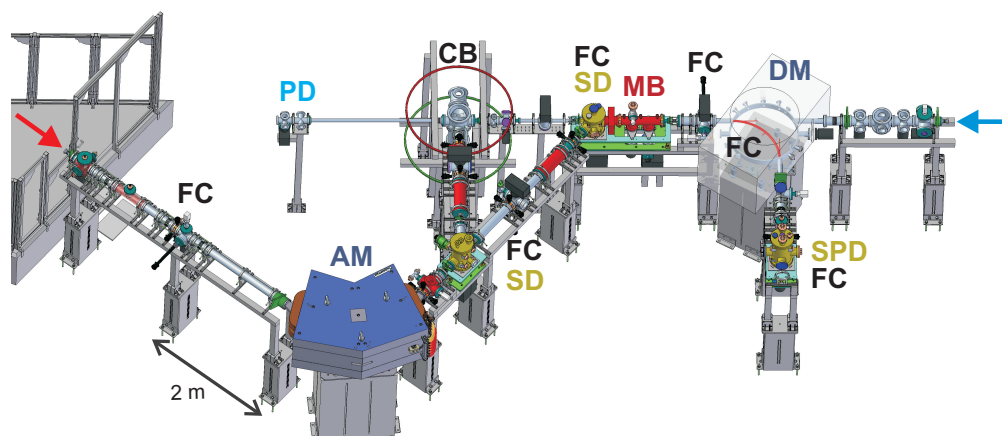


**Figure 1.** Sketch of the photon-ion merged-beams setup PIPE (Photon-Ion spectrometer at the Positron–Electron Tandem-Ring Accelerator (PETRA) III). The photon beam enters the setup from the right (blue arrow) and is parallel to the floor at a nominal height of 2.07 m. It is stopped by a calibrated photodiode (PD) which continuously monitors the absolute photon flux. The ion beam enters from the left (red arrow). It is generated with an ion source that is mounted on a separate platform (not fully shown). The analyzing magnet (AM) provides mass/charge selection of ions for further ion-beam transport. Spherical deflectors (SD) can be used to direct the ions either into the crossed-beams (CB) interaction point or into the merged-beams (MB) collinear beam overlap region. The demerging magnet (DM) deflects primary and product ions out of the photon-beam axis and directs product ions into the single-particle detector (SPD). The ion current can be measured at various places along the ion beamline by inserting Faraday cups (FC) into the ion beam. One FC is mounted inside the DM such that product ions which are deflected by 90° can pass towards the SPD, while ions in different charge states or with different kinetic energies are collected in this FC. The MB is equipped with scanning slits for beam-profile measurements. The figure has been taken from reference [12] (© 2014 IOP Publishing. Reproduced with permission. All rights reserved).
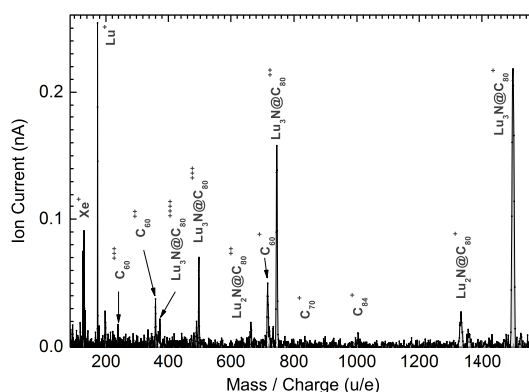


**Figure 2.** Primary-ion mass spectrum with a mixture of $Lu_3N@C_{80}$ (35%) and other fullerenes (65%, mainly $C_{60}$) in the ion source [11]. Well isolated peaks due to singly, doubly, and triply charged intact $Lu_3N@C_{80}$ ions as well as charged fragments are clearly observed. Only one of the peaks is transported further to the photon-ion merged-beams interaction region for a particular photoionization of photofragmentation measurement.

## 3. Results and Discussion

Ion yields of different product ions from photoionization and photofragmentation of initially singly, doubly, and triply charged $Lu_3N@C_{80}$ ions were measured as functions of photon energy. Figure 3 shows results obtained for photon energies in the range 280–330 eV which comprises the threshold for carbon K-shell ionization. The ion yields are all on the same relative cross-section scale. In principle, the photon-ion merged-beams method can be used to determine *absolute* cross sections [3,12]; however, this has not been pursued in the here-discussed experiments due to time constraints.
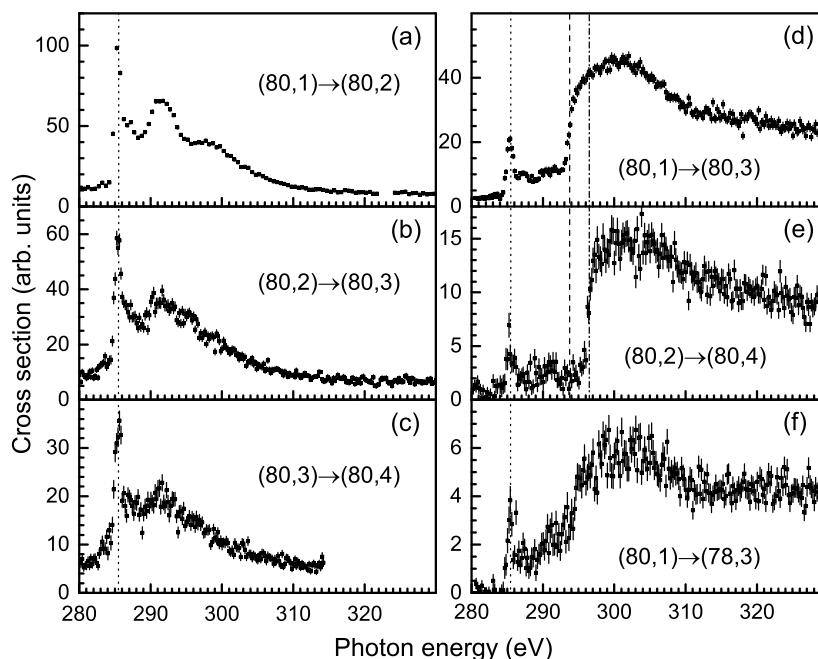


**Figure 3.** Relative cross sections of photo reactions of singly, doubly, and triply charged $Lu_3N@C_{80}$ ions [11]. The short-hand notation $(n, q) \rightarrow (m, r)$ refers to reactions of type $Lu_3N@C_n^{q+} \rightarrow Lu_3N@C_m^{r+}$. The panels (**a**–**c**) on the left show single-ionization results, and the panels (**d**–**f**) on the right show double-ionization data. The dotted line marks the position of the most prominent ionization resonance. It appears at the same energy of $285.4 \pm 0.5$ eV in all channels. The dashed and dash-dotted lines in panels (**d**,**e**) mark the the positions of the carbon K-shell ionization thresholds for the ionization of $Lu_3N@C_{80}^+$ and $Lu_3N@C_{80}^{2+}$, respectively.

The total number of possible product channels is much larger than what is depicted in Figure 3. The majority of the product channels could not be studied, since each of them requires a time-consuming separate measurement. The most comprehensive set of product channels was so far measured for photon interactions with $C_{60}^+$ in the photon-energy range 17–140 eV [6]. It was found that single and double ionization with loss of 0–8 carbon dimers (neutral or ionized $C_2$ molecular fragments) leading to the production of $C_{60-2k}^{r+}$ with $k = 0, 1, \ldots, 8$ and $r = 2, 3$ are the most prominent reaction channels. An analogous range of relevant products channels can also be expected for $Lu_3N@C_{80}$ ions. It must be kept in mind, however, that the photon energies of Figure 3 are at least a factor of two higher than in the above-mentioned study with $C_{60}$ ions, and that, consequently, more reaction channels may be significant. This is particularly true if even higher photon energies of about 1600 eV are applied to reach the Lu M-edge.

The ion-yield spectra at the carbon K-edge (Figure 3) are distinctly different for single ionization on the one hand and for double ionization on the other hand. The single ionization spectra are dominated by resonances that are associated with the excitation of a carbon K-shell electron into unoccupied molecular orbitals and subsequent autoionization. The resonance positions are the same

for all product channels of a given primary ion, and do not change significantly when going from singly to doubly and triply charged Lu$_3$N@C$_{80}$ targets. In contrast, the relative resonance strengths vary markedly when going from one product channel to another. This is due to the different branching ratios into the various reaction channels that are available for the decay of the intermediate resonance states. In addition, distinct threshold features are observed in the double ionization channels. These are not visible in the single-ionization spectra, since the K-hole that is created by the ionization event is rapidly filled by a subsequent Auger process, leading to the emission of a second electron or even more electrons, resulting in double or higher ionization, respectively.

A shift of the threshold energy is observed when going from double ionization of the singly to double ionization of the doubly charged ion (Figure 3d,e). This is due to the additional charge of the product ion and the correspondingly stronger Coulomb attraction of the outgoing photoelectron by the residual ion—as has also been discussed, for example, in the multi-step ionization of rare gas clusters [16,17]. Hellhund et al. [11] used the threshold energy shift to infer the radius of the fullerene shell, and obtained a value of 0.50(4) nm. Within its experimental uncertainty, this value is within the range 0.53–0.56 nm of calculated van-der-Waals radii of C$_{80}$ [18].

It is instructive to compare the ion yields from the photoionization of Lu$_3$N@C$_{80}^+$ with NEXAFS spectra from other carbon-based materials. Such a comparison is presented in Figure 4. Surprisingly, the Lu$_3$N@C$_{80}^+$ spectra are much less structured than the spectra of gas-phase C$_{60}$ [19] and of solid C$_{80}$ [20]. The Lu$_3$N@C$_{80}^+$ spectra more closely resemble the NEXAFS spectrum of graphite [21] when comparing the number and width of resonance features. It is speculated that the electrons of the Sc$_3$N molecular complex strongly hybridize with the electron cloud of the C$_{80}$ cage, since a strong chemical interaction between fullerene cage and chemical content could wash out the photoionization resonance structure of the carbon cage. It would also provide an explanation for the remarkable stability of this and similar endohedral fullerene species (e.g., Sc$_3$N@C$_{80}$ [7]), as it also manifests itself in the mass/charge spectrum of Figure 2, where there are no prominent mass peaks from charged Lu$_3$N@C$_{80}^+$ fragments containing less than 80 carbon atoms. More insight into these issues could possibly be provided by supporting theoretical calculations.
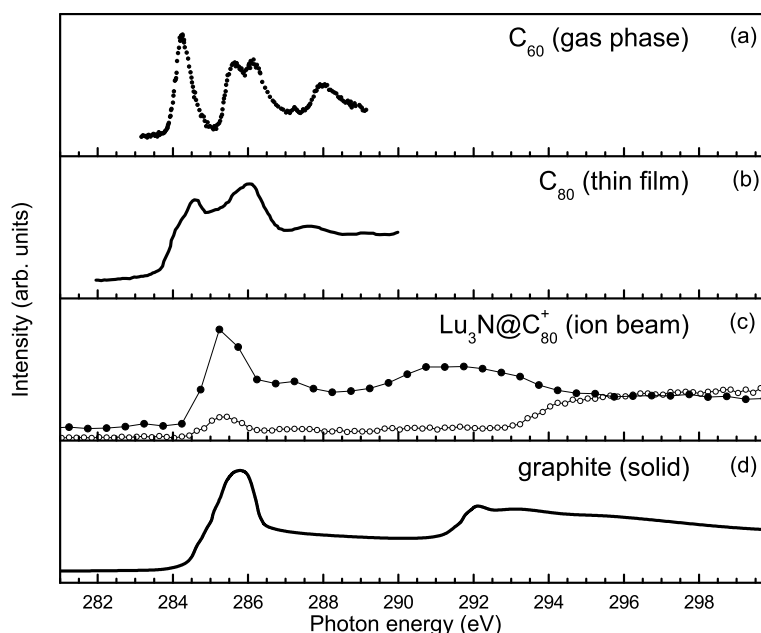


**Figure 4.** Comparison of the results for ionization of (**c**) Lu$_3$N@C$_{80}^+$ (● single ionization from Figure 3a, ○ double ionization from Figure 3d) with photoabsorption in other carbon-based materials—i.e., (**a**) C$_{60}$ vapor [19]; (**b**) C$_{80}$ evaporated as a thin film onto a solid substrate [20]; and (**d**) graphite [21]. The figure has been adapted from [11].

In addition to the energy range of the carbon K-edge, also the energy ranges 390–450 eV and 1500–1700 eV of the N K-edge and the lowest Lu M-edge, respectively, were scrutinized [11]. Ion-yield spectra (which are not displayed here) were taken for heavy photo products ranging from $Lu_3N@C_{80}^{3+}$ to $Lu_3N@C_{72}^{5+}$ and $Lu_3N@C_{74}^{6+}$. None of the corresponding spectra exhibited any sign of these edges. Most probably, the absorption of an energetic 1600-eV photon by one of the Lu atoms leads to a much more violent fragmentation event, such that large fragments cannot be observed. This is interesting, for example, from a radiobiological point of view, and will be more closely investigated in future follow-up experiments where lower-mass fragments will hopefully be detected.

## 4. Conclusions

Inner-shell ionization of endohedral fullerenes in the gas phase has been achieved for the first time [11] by using a very sensitive photon-ion merged-beams method which provides information similar to NEXFAS, albeit with the additional possibility to discriminate between different product channels. This has become possible by combining state-of-the-art ion-beam-technology with XUV radiation from the world's brightest 3rd generation synchrotron light-source. This has opened a door to future studies with other rare gas-phase nanomaterials such as biomolecular ions and size-selected cluster ions.

**Conflicts of Interest:** The author declares no conflict of interest. The founding sponsors had no role in the design of the study; in the collection, analyses, or interpretation of data; in the writing of the manuscript, and in the decision to publish the results.

## Abbreviations

The following abbreviations are used in this manuscript:

| | |
|---|---|
| ALS | Advanced Light Source |
| ECR | Electron Cyclotron Resonance |
| EXAFS | Extended X-ray Absorption Fine-Structure |
| NEXAFS | Near-Edge X-ray Absorption Fine Structure |
| PIPE | Photon-Ion Spectrometer at PETRA III |

## References

1. Popov, A.A.; Yang, S.; Dunsch, L. Endohedral fullerenes. *Chem. Rev.* **2013**, *113*, 5989–6113.
2. Katayanagi, H.; Kafle, B.P.; Kou, J.; Mori, T.; Mitsuke, K.; Takabayashi, Y.; Kuwahara, E.; Kubozono, Y. The $4d$–$4f$ dipole resonance of the Pr atom in an endohedral metallofullerene, $Pr@C_{82}$. *J. Quant. Spectrosc. Radiat. Transf.* **2008**, *109*, 1590–1598.
3. Schippers, S.; Kilcoyne, A.L.D.; Phaneuf, R.A.; Müller, A. Photoionization of ions with synchrotron radiation: From ions in space to atoms in cages. *Contemp. Phys.* **2016**, *57*, 215–229.
4. Scully, S.W.J.; Emmons, E.D.; Gharaibeh, M.F.; Phaneuf, R.A.; Kilcoyne, A.L.D.; Schlachter, A.S.; Schippers, S.; Müller, A.; Chakraborty, H.S.; Madjet, M.E.; et al. Photoexcitation of a volume plasmon in $C_{60}$ ions. *Phys. Rev. Lett.* **2005**, *94*, 065503.
5. Bilodeau, R.C.; Gibson, N.D.; Walter, C.W.; Esteves-Macaluso, D.A.; Schippers, S.; Müller, A.; Phaneuf, R.A.; Aguilar, A.; Hoener, M.; Rost, J.M.; et al. Single-photon multiple detachment in fullerene negative ions: Absolute ionization cross sections and the role of the extra electron. *Phys. Rev. Lett.* **2013**, *111*, 043003.
6. Baral, K.K.; Aryal, N.B.; Esteves-Macaluso, D.A.; Thomas, C.M.; Hellhund, J.; Lomsadze, R.; Kilcoyne, A.L.D.; Müller, A.; Schippers, S.; Phaneuf, R.A. Photoionization and photofragmentation of the $C_{60}^{+}$ molecular ion. *Phys. Rev. A* **2016**, *93*, 033401.

7. Müller, A.; Schippers, S.; Phaneuf, R.A.; Habibi, M.; Esteves, D.; Wang, J.C.; Kilcoyne, A.L.D.; Aguilar, A.; Yang, S.; Dunsch, L. Photoionization of the endohedral fullerene ions $Sc_3N@C_{80}^+$ and $Ce@C_{82}^+$ by synchrotron radiation. *J. Phys. Conf. Ser.* **2007**, *88*, 012038.

8. Müller, A.; Schippers, S.; Habibi, M.; Esteves, D.; Wang, J.C.; Phaneuf, R.A.; Kilcoyne, A.L.D.; Aguilar, A.; Dunsch, L. Significant redistribution of Ce 4d oscillator strength observed in photoionization of endohedral $Ce@C_{82}^+$ ions. *Phys. Rev. Lett.* **2008**, *101*, 133001.

9. Kilcoyne, A.L.D.; Aguilar, A.; Müller, A.; Schippers, S.; Cisneros, C.; Alna'Washi, G.; Aryal, N.B.; Baral, K.K.; Esteves, D.A.; Thomas, C.M.; et al. Confinement resonances in photoionization of $Xe@C_{60}^+$. *Phys. Rev. Lett.* **2010**, *105*, 213001.

10. Phaneuf, R.A.; Kilcoyne, A.L.D.; Aryal, N.B.; Baral, K.K.; Esteves-Macaluso, D.A.; Thomas, C.M.; Hellhund, J.; Lomsadze, R.; Gorczyca, T.W.; Ballance, C.P.; et al. Probing confinement resonances by photoionizing Xe inside a $C_{60}^+$ molecular cage. *Phys. Rev. A* **2013**, *88*, 053402.

11. Hellhund, J.; Borovik, A., Jr.; Holste, K.; Klumpp, S.; Martins, M.; Ricz, S.; Schippers, S.; Müller, A. Photoionization and photofragmentation of multiply charged $Lu_3N@C_{80}$ ions. *Phys. Rev. A* **2015**, *92*, 013413.

12. Schippers, S.; Ricz, S.; Buhr, T.; Borovik, A., Jr.; Hellhund, J.; Holste, K.; Huber, K.; Schäfer, H.J.; Schury, D.; Klumpp, S.; et al. Absolute cross sections for photoionization of $Xe^{q+}$ ions ($1 \leq q \leq 5$) at the 3d ionization threshold. *J. Phys. B* **2014**, *47*, 115602.

13. Viefhaus, J.; Scholz, F.; Deinert, S.; Glaser, L.; Ilchen, M.; Seltmann, J.; Walter, P.; Siewert, F. The variable polarization XUV beamline P04 at PETRA III: Optics, mechanics and their performance. *Nucl. Instrum. Methods A* **2013**, *710*, 151–154.

14. Milosavljević, A.R.; Giuliani, A.; Nicolas, C. Gas-phase near-edge X-ray absorption fine structure (NEXAFS) spectroscopy of nanoparticles, biopolymers, and ionic species. In *X-ray and Neutron Techniques for Nanomaterials Characterization*; Kumar, C.S., Ed.; Springer: Berlin/Heidelberg, Germany, 2016; pp. 451–505.

15. Trassl, R. ECR ion sources. In *The Physics of Multiply and Highly Charged Ions. Volume 1: Sources, Applications and Fundamental Processes*; Currell, F., Ed.; Kluwer Academic Publishers: Dordrecht, The Netherlands, 2003; pp. 3–37.

16. Bostedt, C.; Thomas, H.; Hoener, M.; Eremina, E.; Fennel, T.; Meiwes-Broer, K.H.; Wabnitz, H.; Kuhlmann, M.; Plönjes, E.; Tiedtke, K.; et al. Multistep ionization of argon clusters in intense femtosecond extreme ultraviolet pulses. *Phys. Rev. Lett.* **2008**, *100*, 133401.

17. Arbeiter, M.; Fennel, T. Ionization heating in rare-gas clusters under intense XUV laser pulses. *Phys. Rev. A* **2010**, *82*, 013201.

18. Adams, G.B.; O'Keeffe, M.; Ruoff, R.S. Van der Waals surface areas and volumes of fullerenes. *J. Phys. Chem.* **1994**, *98*, 9465–9469.

19. Krummacher, S.; Biermann, M.; Neeb, M.; Liebsch, A.; Eberhardt, W. Close similarity of the electronic structure and electron correlation in gas-phase and solid $C_{60}$. *Phys. Rev. B* **1993**, *48*, 8424–8429.

20. Cummins, T.R.; Bürk, M.; Schmidt, M.; Armbruster, J.F.; Fuchs, D.; Adelmann, P.; Schuppler, S.; Michel, R.H.; Kappes, M.M. Electronic states and molecular symmetry of the higher fullerene $C_{80}$. *Chem. Phys. Lett.* **1996**, *261*, 228–233.

21. Terminello, L.; Shuh, D.; Himpsel, F.; Lapiano-Smith, D.; Stöhr, J.; Bethune, D.; Meijer, G. Unfilled orbitals of $C_{60}$ and $C_{70}$ from carbon K-shell X-ray absorption fine structure. *Chem. Phys. Lett.* **1991**, *182*, 491–496.